



An acid-doped ice membrane for selective proton transport

Tom Sleutels¹  | Iosif Kaniadakis¹ | Olaniyi Oladimeji¹ |
Harm van der Kooij¹ | Annemiek ter Heijne²  | Michel Saakes¹

¹Wetsus, European Centre of Excellence for Sustainable Water Technology, Leeuwarden, The Netherlands

²Environmental Technology, Wageningen University, Wageningen, The Netherlands

Correspondence

Annemiek ter Heijne, Environmental Technology, Wageningen University, Bornse Weiland 9, 6708 WG Wageningen, The Netherlands.
Email: annemiek.terheijne@wur.nl

Funding information

European Union's Horizon 2020 Research and Innovation program, Grant/Award Number: 731187

Summary

Cation exchange membranes need to have high permselectivity for protons to make these membranes suitable for, for example, energy storage devices. Here, we present the proof of concept for a proton selective membrane made of hydrochloric acid-doped ice. The proton selectivity of this acid-doped ice membrane is the result of defects in the ice structure, caused by the acid. Ice membranes were made from different hydrochloric acid concentrations (0.1–2.0 M). The proton permselectivity of all ice membranes was above 99.7% when both Na^+ and K^+ were present. The resistivity decreased exponentially with the concentration of acid in the ice membrane, reaching a value of $12 \Omega\cdot\text{cm}$. The ice membranes were tested in an electrochemical cell using the Fe/Fe^{2+} and $\text{Fe}^{2+}/\text{Fe}^{3+}$ redox couples, and a power density of 7 W/m^2 and OCV of 0.87 V were measured. The resistance of the ice membrane increased with time as protons moved from the ice structure, as determined from the higher pH of the ice after melting. These expelled protons (and corresponding counter charged ions) were not replaced by other mobile cations, indicating a permanent loss in conductivity, but not selectivity. To apply the ice membrane as a selective separator for protons in energy storage devices in the future, the membrane thickness should be reduced and the protons should be retained inside the ice.

KEYWORDS

energy storage, ice, IEM, proton exchange membrane

1 | INTRODUCTION

Renewable energy technologies such as wind and solar power are facing the problem of matching irregular production with fluctuating demand. Storage of (large quantities) of electrical energy is very much in need to dampen this difference in supply and demand. One popular evolving solution is the development of concentration gradient batteries, which are electrochemical storage technologies in which the electrical charge is

stored in a concentration difference of ions. For example, the electricity produced by renewables can be used for the formation of a pH gradient in the acid-base-flow battery.^{1,2} In this acid-base battery, water is dissociated into protons and hydroxide ions by the use of a bipolar membrane, while charging the battery. In this way, electrical energy is stored in a proton gradient. The energy stored in this proton gradient can be harvested by recombining the protons and hydroxyl in the junction of the bipolar membrane in a process called reverse

This is an open access article under the terms of the Creative Commons Attribution License, which permits use, distribution and reproduction in any medium, provided the original work is properly cited.

© 2020 The Authors. *International Journal of Energy Research* published by John Wiley & Sons Ltd

electrodialysis. Other examples are water-based batteries that make use of two different redox couples, for example, all vanadium batteries, the Fe-Cr battery and the Ce-V battery.³⁻⁶

Successful application of many electrochemical storage technologies relies on selectively moving ions through the membrane at the lowest possible energy loss.⁷⁻⁹ However, all ion exchange membranes (both heterogeneous and homogeneous) suffer from processes such as co-ion and water transport and swelling, which after many charge/discharge cycles lead to high energetic losses and low cycle efficiencies as ions of the redox couples get mixed.⁹⁻¹¹

The challenge of non-ideal permselectivity of ion exchange membranes in electrochemical cells has created the need for further research into alternative materials for such membranes. A membrane consisting of ice could serve this purpose.

In solid state, water is a poor conductor of electricity due to the presence of few ions in the molecular structure, and hence ice has a high ionic resistance. However, the conductivity of ice can be enhanced by altering the mobility of ions in the crystal structure by introducing defects in the molecular ice structure. Four types of defects have been identified as charge carriers in the structure of ice namely H_3O^+ , OH^- , Bjerrum L and D-defects.¹² In the Bjerrum L defect, the hydrogen bond in water has no proton, while in the Bjerrum D defect the hydrogen bond in water has two protons. The first two defects (H_3O^+ , OH^-) enable ions to move through the transfer of protons from one end of a hydrogen bond to the neighbouring water molecule. In both Bjerrum defects, protons move through the rotation of a water molecule and the protons hop from one water bond to the next one through the Grotthuss mechanism.¹³ The conductivity in doped ice is assumed to be controlled by the free migration of L defects.¹⁴

The defects are the ionic charge carriers in ice and can be introduced by incorporating impurities in the crystal structure of ice, which is known as doping. Acids (HF, HCl), ammonia (NH_3), potassium hydroxide (KOH), sodium hydroxide (NaOH) and their derivatives like ammonium fluoride (NH_4F) or potassium chloride (KCl) cannot only be incorporated into the ice crystal, but they can also alter the protonic charge carrier concentration in the ice, creating a charged ice structure.¹⁵ By doping the ice with different concentrations of acid, the charge density of the solid ice structure can be altered.¹⁶ Due to the presence of the defects inside the ice, protons can hop from defect to defect and thereby move through the ice. Other cations, however, are not able to move through these defects and therefore, theoretically, the ice would behave like the perfect proton exchange membrane.¹⁷

The aim of this study is to show a proof-of-principle of an acid-doped ice membrane that is 100% permselective for protons and made of ice, which does not transport water or co-ions. These ice membranes were produced by incorporating HCl into the crystal structure of ice made by freezing the acid solution. The permselectivity and resistivity of the resulting ice membrane were tested in an electrochemical cell, and its capacity for application in electrochemical energy storage systems was demonstrated in polarization curves.

2 | MATERIALS AND METHODS

2.1 | Design of the cell

A poly methyl methacrylate (PMMA) cell with a plastic frame in the middle was used for the experiments. This plastic frame contained a window (6.3 cm^2 ; Figure 1), which contained a manifold that holds eight parallel Ti tubes of 3 mm outer diameter and 2 mm inner diameter. These tubes were connected to a cryostat at the outside of the chamber and were used to transport cooling liquid. The liquid cooling agent was glycol (freezing temperature -40°C) that was diluted to approx. -26°C as maximum freezing temperature to have a lower viscosity for pumping through the Ti tubes. The cell was placed inside a temperature-controlled chamber at 272 K (ICP260, temperature range -12°C to $+60^\circ\text{C}$, Memmert GmbH, Schabach, Germany).

2.2 | Ice membrane composition and freezing conditions

Five different ice membranes were used for comparison (Table 1). Ice formation was controlled by controlling the temperature of the cooling glycol liquid inside the tubes in the window. The freezing points of the acid solutions were calculated from the freezing point depression of the solvent (water) using the Clausius-Clapeyron equation and Raoult's law.

$$\text{Freezing point}_{\text{acid solution}} = \text{Freezing point}_{\text{solvent}} - \Delta T_f, \quad (1)$$

where the freezing point of the solvent (water) is 0°C . The freezing point depression for water can be calculated using¹⁸

$$\Delta T_f = K_f * m * i, \quad (2)$$

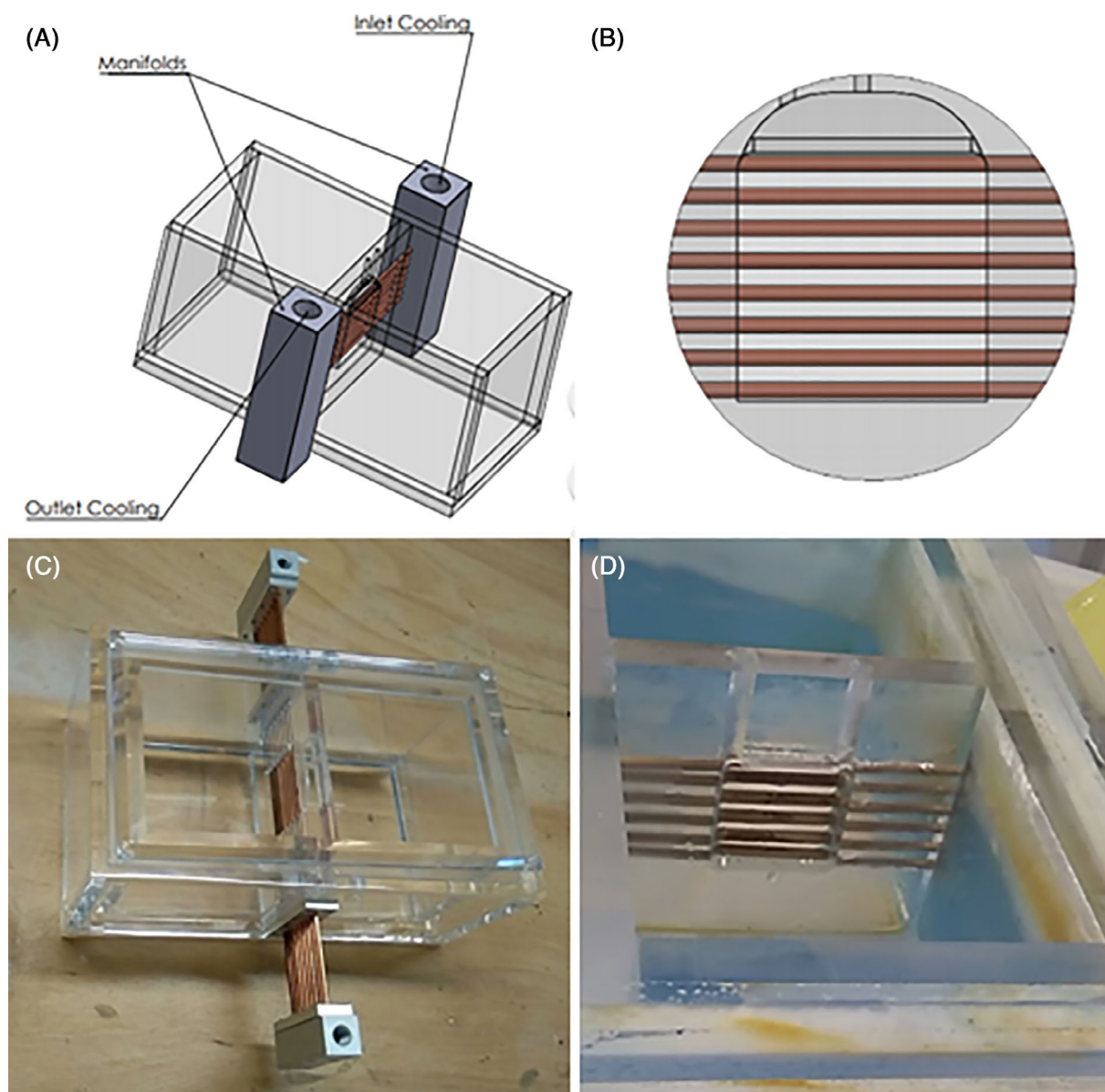


FIGURE 1 Schematic (A) and photograph (C) of the cell with the frame in the middle containing the window and manifold with Cu tubes. In this cell still Cu tubes were used, however these Cu tubes were sensitive to corrosion and were replaced later on by Ti tubes grade 1 (outer diameter 3.0 mm, inner diameter 2.0 mm). Schematic (B) and photograph (D) of the window and manifold containing the cooling tubes [Colour figure can be viewed at wileyonlinelibrary.com]

TABLE 1 Calculated freezing points of acid solutions and the practically applied temperatures

Concentration of acid (M)	% Weight	Freezing point ($^{\circ}\text{C}$)	Applied temperatures ($^{\circ}\text{C}$)
0	0	0.0	-1
0.1	0.37	-0.35	-2
0.25	0.91	-0.90	-3
0.5	1.8	-1.9	-4
1	3.7	-4.0	-8
2	7.3	-9.4	-15

where m is the molality of the solute, K_f is the cryoscopic constant (1.86 K kg/mol for the freezing point of water), i is the Van't Hoff factor (this factor is 2 since HCl is completely dissociated). This equation is valid for ideal solutions and therefore equations for non-ideal solutions can be found in the supporting information.

The cooling cryostat system (Thermo Scientific Haake A10) was set some degrees lower than the calculated freezing point depression. For example, for 1 M HCl, the cryostat temperature was set at -8°C while the climate chamber temperature was 0.5°C . The measured temperature of the liquids inside the electrochemical cell was -2.6°C , which is 1.4°C above the calculated freezing temperature of 1 M HCl solution.

2.3 | Permselectivity test

To test the permselectivity of the ice membrane, the compartment on one side of the ice was filled with acid with the same concentration as the ice, while the other side was filled with acid with a concentration 10 times lower than the ice. A lower acidity of the electrolyte is required as the ice would otherwise melt due to the difference in freezing temperature at higher acidity. For the permselectivity test, 0.1 M KCl and 0.1 M NaCl were added to the compartment with the lower acidity. The permselectivity of the 2 M ice membrane was not determined due to experimental difficulties related to the required cryostat temperature of -15°C . This low freezing temperature was required because of non-ideal behaviour of a solution with such a high concentration of acid. The low temperature of -15°C made that the liquids in the compartments started freezing as well.

Permselectivity of the ice membrane was tested by measuring the concentrations of K^+ and Na^+ in both compartments. The change in cation concentrations in both compartments was followed for 24 hours by taking liquid samples. Also, the ions inside the membrane, after melting of the ice, were analysed. The permselectivity φ^m was calculated using¹⁹

$$\varphi^m = \frac{T_{\text{cou}}^m - T_{\text{cou}}^s}{T_{\text{co}}^s}, \quad (3)$$

where T_{cou}^m and T_{cou}^s are the transport numbers of the counter-ions in the membrane, and T_{co}^s the co-ions in solution.

2.4 | Resistance

The ohmic resistance of the ice membrane was determined using high frequency (1000 Hz) Direct Impedance

measurement with a HIOKI BT3563 battery tester across two Pt/Ir Ti-mesh electrodes (Magneto Anodes B.V., Schiedam). The specific resistance or resistivity (R_s ; $\Omega\cdot\text{cm}$) of the membrane, which represents the material property, was estimated from the area resistance and the membrane thickness; δ .

$$R_s = \frac{R_A}{\delta}. \quad (4)$$

2.5 | Power density and polarization curves

Polarization curves have been recorded using an Ivium VERTEX potentiostat (IVIUM, Eindhoven, the Netherlands) for ice membranes made of 0.1, 0.5, 1.0 and 2.0 M HCl by changing the cell voltage in steps of 0.1 V and recording the resulting current density for 60 seconds (the final reading was used). The redox couples were $\text{Fe}^{3+}/\text{Fe}^{2+}$ (catholyte) and $\text{Fe}^{2+}/\text{Fe(s)}$ (anolyte) in concentrations of 250 mM. The electrodes consisted of Pt/Ir 70:30 Ti-mesh 1.0 (Magneto Anodes B.V., Schiedam, The Netherlands) and solid iron. For the 2 M HCl ice membrane, a galvanostatic scan was done with a scan rate of 0.1 mA/s directly after formation of the ice membrane as the 2 M HCl ice was more difficult to prepare. The temperature needed for ice formation was -9.4°C for the electrolyte as calculated using the simplified Equation (2). In reality, the cryostat was cooled to -15°C , making the ice formation more difficult to control, which resulted in a thicker membrane than wanted (Table 3).

The power density (P_d ; W/m^2) was calculated from the cell voltage (E_{cell} ; V) and current density I_d (A/m^2) using

$$P_d = I_d E_{\text{cell}}. \quad (5)$$

The maximum power density (P_{max} ; W/m^2) was calculated using¹¹

$$P_{\text{max}} = \frac{\text{OCV}^2}{4RA}, \quad (6)$$

where OCV is the open cell voltage (V), R is the membrane resistance (Ω) and A is the area of the membrane (6.3 cm^2).

2.6 | Analysis

Na^+ and K^+ concentrations in both compartments were analysed using a Metrohm Compact IC Flex 930 instrument with a cation column (Metrosep C 4-150/4.0).

The pH was measured using two 12 mm diameter glass pH electrodes especially calibrated for low pH. The calibration for pH 1 required a buffer solution of 0.2 M KCl diluted into 0.2 M HCl at 298 K for correction of the activity of protons.

3 | RESULTS AND DISCUSSION

3.1 | Ice membrane freezing procedure

To create the ice membrane, the cell was filled with a solution with the desired concentration of hydrochloric acid of 0.1, 0.5, 1.0 or 2.0 M HCl solution (Table 1). The parallel set of eight Ti tubes of the manifold initiated the formation of ice locally by carrying the cooling agent inside. Due to the cooling power from the cryogenic bath, an initial ice layer was formed around the cooling tubes first, while the remaining part of the acid remained liquid. Cooling was continued until the entire window between the tubes was filled with ice and the cell was completely separated into two compartments (Figure 1). To make sure that the window dividing the two compartments was fully formed, some of the acid solution from either of the two sides of the cell was removed and the ice membrane was considered complete if the liquid level in the opposite compartment remained the same. In about 1 day, the membranes of pure water, 0.1 M HCl and 0.5 M HCl reached a thickness of about 2 cm, which could be maintained (Table 3). However, the membranes of 1 and 2 M HCl were much thicker; 3.8 cm for 1 M and 7 cm for 2 M. Due to the lower freezing temperature at these high acid concentrations, the freezing process was more difficult to control, as the difference between the temperature of the cooling liquid in the tubes and the temperature of the surrounding electrolyte is higher. These ice membranes are much thicker than commercial cation exchange membranes, which are in the order of $\sim 100 \mu\text{m}$.²⁰

The energy needed for cooling of the ice and pumping of the cooling agent through the Ti tubes needs to be minimized to make the ice membrane a viable alternative to classical ion exchange membranes, and insulation is therefore crucial. In our situation, we therefore used an insulated thermal chamber that was kept at a temperature slightly above the freezing temperature of the ice (temperature difference for 1 M HCl ice was 5.9°C between the temperature of the thermal chamber and the cryostat temperature). Narrowing down this temperature difference and improving the insulation of the thermal chamber will decrease the energy needed for maintaining the ice. Another requirement to lower the energy losses is to lower the

viscosity of the cooling agent that passes the Ti tubes, thereby reducing the required pumping energy.

3.2 | Permselectivity

The permselectivity of the ice membranes of different acid concentrations was determined using NaCl and KCl in the compartment with 10 times lower acid concentration compared to the ice membrane, and the same acid concentration as the ice membrane in the other compartment. Figure 2 shows this permselectivity after 24 hours. For each ice membrane, the proton permselectivity was higher than 99.7% when K^+ was present and higher than 99.8% when Na^+ was present. The permselectivity for protons of the ice membrane is considerably higher than the permselectivity of 99% for commercial CEMs,²⁰ however, these membranes may also have higher permselectivity when they are thicker.

3.3 | Power density

Polarization curves were recorded for membranes made of 0.1, 0.5, 1.0 M and 2.0 M HCl (Figure 3 and Table 2). The open cell voltage (OCV) is the maximum voltage that can be harvested from the electrode reactions and should ideally be close to the theoretical values. The OCV was determined by adding two reference electrodes (Ag/AgCl) close to the ice membrane.

The OCV was stable around 0.87 V for all membranes using $\text{Fe}^{3+}/\text{Fe}^{2+}$ vs Fe^{2+}/Fe as redox couples, for which the theoretical voltage ranges from 0.83 (-13°C) to 0.88 V (-3°C) as calculated from the Nernst equation.

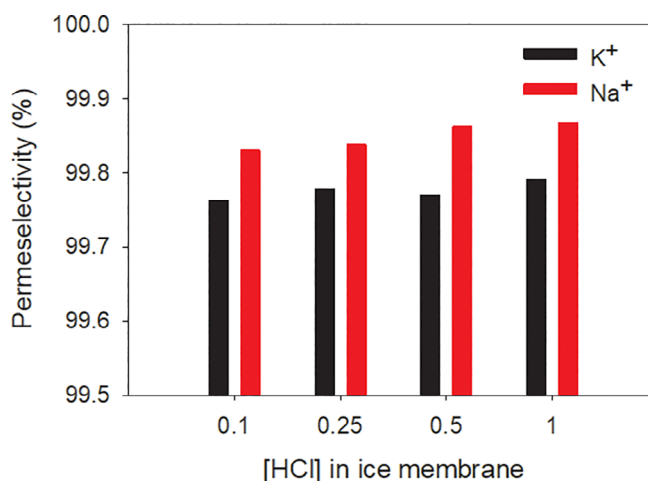


FIGURE 2 Permselectivity using Na^+ and K^+ distribution vs molarity in acid-doped ice. The y-axis scale is between 99.5 and 100.0% [Colour figure can be viewed at wileyonlinelibrary.com]

The maximum current density (short circuit current) increased from 10 A/m² for the 0.1 M HCl membrane to 34 A/m² for the 2 M HCl membrane. The maximum power density was 7 W/m² for the 2 M HCl membrane. It must be emphasized that the membranes were several centimetres thick, and when the thickness of the ice membrane can be reduced, the power density increases significantly. For the ice membrane to be used in an energy storage device, ideally the thickness should be reduced to a value below 1 cm using thinner Ti tubes. Thinner Ti tubes will require a lower viscosity cooling agent to keep the pressure across the Ti tubes acceptable while pumping. The pumping energy and the energy

needed for cooling of the ice membrane have to be minimized in further technical development of an ice-separated battery in order to increase the round trip efficiency.

3.4 | Resistivity and area resistance

The resistivity and area resistance of the ice membranes were determined using direct impedance measurements (Table 3). The resistivity was determined as it is independent of the thickness of the membrane. Both resistivity and area resistance decreased exponentially with the concentration of hydrochloric acid in the ice membrane. Since proton concentration increases the membrane conductivity, the resistance of the ice is expected to decrease.¹⁶ The lowest measured resistivity was 12 Ω.cm for a 2 M HCl ice membrane. This 2 M HCl ice membrane also had the lowest area resistance; 47 Ω.cm² for the 2 M HCl ice membrane. This resistance is still high compared to commercial CEMs. This high resistance is mostly due to the membrane thickness; this membrane had a thickness of 7 cm, whereas the others were close to 2 cm. More controlled freezing should result in a reduction of this thickness and consequently in a lower area resistance. For example, a thermocouple could be used to control the temperature more accurately and thereby control the freezing process of the ice membrane.

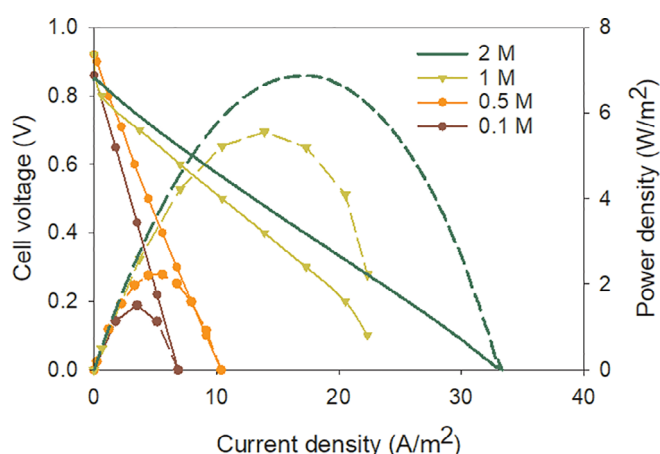


FIGURE 3 Polarisation and power curves for acid membranes of 0.1, 0.5, 1 and 2 M HCl [Colour figure can be viewed at wileyonlinelibrary.com]

TABLE 2 Open cell voltage and maximum power densities of the ice membranes

[HCl] in membrane (M)	Open cell voltage (V)	Max power density (W/m ²)
0.1	0.86	1.5
0.5	0.91	2.3
1	0.85	5.6
2	0.82	7.0

TABLE 3 Experimentally determined thickness, resistance and resistivity

[HCl] in membrane (M)	Thickness (cm)	Resistance (Ω.cm ²)	Resistivity (Ω.cm)
0	2.8	1608·10 ³	574·10 ³
0.1	1.2	4.6·10 ³	0.57·10 ³
0.5	1.9	0.47·10 ³	90
1.0	3.8	81	21
2.0	7	47	12

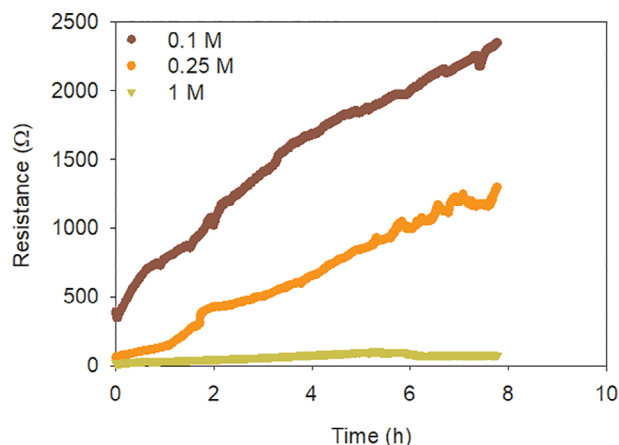


FIGURE 4 Change in resistance of the ice membrane (0.1, 0.5 and 1 M) in time measured by direct impedance at $f = 1000$ Hz [Colour figure can be viewed at wileyonlinelibrary.com]

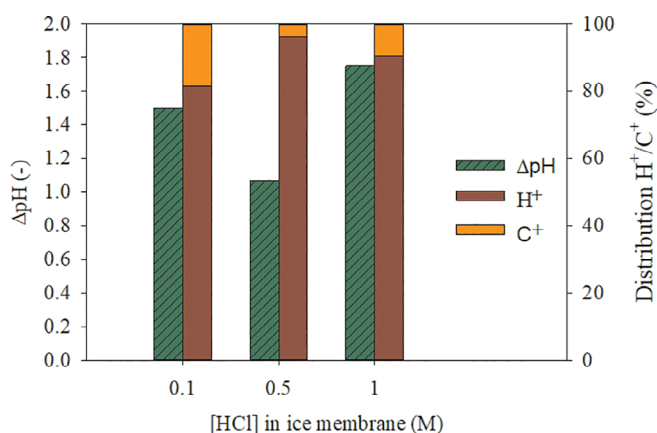


FIGURE 5 Change in pH of the ice membrane before and after use. Also, the composition of the ice membrane after melting is given. Total concentration of protons and other cations (shown as C^+) is shown [Colour figure can be viewed at wileyonlinelibrary.com]

separated by freezing a salt solution; pure water and pure salt are then obtained.²¹ This resistance increase was the most prominent for the 0.1 M ice membrane, as it contained fewest protons, while the increase was only minor for the 1 M ice membrane, as it contained most protons. Nevertheless, on the long term also an increase in resistance for the higher concentration ice membranes can be expected.

To confirm if proton diffusion out of the membrane was the reason for the resistance increase, the ice was melted after the experiment and the pH of the remaining liquid was measured. Figure 5 shows the pH change (before and after melting the ice membrane) for the different membranes, which was between 1 and 1.7 pH units. From this change in pH, the number of protons that have been

removed from the ice membrane was calculated, assuming the ice thickness did not change during the experiment. At the same time, K^+ and Na^+ concentrations were measured, to assess if these had entered the ice structure (C^+ in Figure 5). This analysis shows that a maximum of 20% of the protons that diffused from the membrane were replaced by other cations. The other protons that diffused from the membrane were accompanied by a loss in Cl^- ions from the ice structure (balancing charge for the protons) and therefore represent a permanent loss in charge from the ice structure. Future research should, therefore, focus on retaining the protons inside the ice structure to maintain a low resistance and high permselectivity.

4 | CONCLUSIONS

In this work, we demonstrate, for the first time, the formation of an acid-doped ice membrane. By freezing an acid solution, a layer of ice is created that only allows the transport of protons with a permselectivity higher than 99.7%. This selective proton transport has promising application in energy storage devices like the acid-base battery. The resistance of this membrane can be decreased by increasing the acid concentration in the membrane. One major challenge is that, over time, the acid is expelled from the membrane and the membrane resistance increases. Therefore, besides reducing the thickness of the ice layer, focus should be on retaining the protons inside the membrane. Ice membrane thickness can be reduced by using thinner cooling tubes and a more controlled freezing procedure.

ACKNOWLEDGEMENTS

This work was performed in the cooperation framework of Wetsus, European Centre of Excellence for Sustainable Water Technology, within the BAoBaB project. Wetsus is co-funded by the Dutch Ministry of Economic Affairs and Ministry of Infrastructure and Environment, the Province of Fryslân, and the Northern Netherlands Provinces (www.wetus.eu). The BAoBaB project (“Blue acid/base battery: Storage and recovery of renewable electrical energy by reversible salt-water dissociation”) has received funding from the European Union's Horizon 2020 Research and Innovation program under Grant Agreement no. 731187 (www.baobabproject.eu). The authors would like to thank Dr. Antoine Kemperman for critical reading of the manuscript.

DATA AVAILABILITY STATEMENT

The data that support the findings of this study are openly available in DANS-EASY database at <https://doi.org/10.17026/dans-xf-zd8n>

ORCID

Tom Sleutels  <https://orcid.org/0000-0001-8251-7879>

Annemiek ter Heijne  <https://orcid.org/0000-0002-6882-8395>

REFERENCES

1. Walther JF. Process for production of electrical energy from the neutralization of acid and base in a bipolar membrane cell; 1980. <https://patents.google.com/patent/US4311771A/en>. Accessed March 1, 2019.
2. Van Egmond WJ, Saakes M, Porada S, Meuwissen T, Buisman CJN, Hamelers HVM. The concentration gradient flow battery as electricity storage system: technology potential and energy dissipation. *J Power Sources*. 2016;325:129-139. <https://doi.org/10.1016/j.jpowsour.2016.05.130>.
3. Fang B, Iwasa S, Wei Y, Arai T, Kumagai M. A study of the Ce(III)/Ce(IV) redox couple for redox flow battery application. *Electrochim Acta*. 2002;47:3971-3976. [https://doi.org/10.1016/S0013-4686\(02\)00370-5](https://doi.org/10.1016/S0013-4686(02)00370-5).
4. Lopez-Atalaya M, Codina G, Perez JR, Vazquez JL, Aldaz A. Optimization studies on a Fe/Cr redox flow battery. *J Power Sources*. 1992;39:147-154. [https://doi.org/10.1016/0378-7753\(92\)80133-V](https://doi.org/10.1016/0378-7753(92)80133-V).
5. Skyllas-Kazacos M, Kasherman D, Hong DR, Kazacos M. Characteristics and performance of 1 kW UNSW vanadium redox battery. *J Power Sources*. 1991;35:399-404. [https://doi.org/10.1016/0378-7753\(91\)80058-6](https://doi.org/10.1016/0378-7753(91)80058-6).
6. Aurbach D, Gofer Y, Lu Z, et al. A short review on the comparison between Li battery systems and rechargeable magnesium battery technology. *J Power Sources*. 2001;97-98:28-32. [https://doi.org/10.1016/S0378-7753\(01\)00585-7](https://doi.org/10.1016/S0378-7753(01)00585-7).
7. Nijmeijer K, Metz S. Chapter 5 Salinity gradient energy. *Sustainability Science and Engineering*. Amsterdam, The Netherlands: Elsevier; 2010. [https://doi.org/10.1016/S1871-2711\(09\)00205-0](https://doi.org/10.1016/S1871-2711(09)00205-0).
8. Zlotorowicz A, Strand RVV, Burheim OSS, Wilhelmsen SK, Wilhelmsen Ø, Kjelstrup S. The permselectivity and water transference number of ion exchange membranes in reverse electrodialysis. *J Membr Sci*. 2017;523:402-408. <https://doi.org/10.1016/j.memsci.2016.10.003>.
9. Tedesco M, Hamelers HVM, Biesheuvel PM. Nernst-Planck transport theory for (reverse) electrodialysis: I. Effect of co-ion transport through the membranes. *J Membr Sci*. 2016;510:370-381. <https://doi.org/10.1016/j.memsci.2016.03.012>.
10. Tedesco M, Scalici C, Vaccari D, Cipollina A, Tamburini A, Micale G. Performance of the first reverse electrodialysis pilot plant for power production from saline waters and concentrated brines. *J Membr Sci*. 2016;500:33-45. <https://doi.org/10.1016/j.memsci.2015.10.057>.
11. Veerman J, Post JWW, Saakes M, Metz SJJ, Harmsen GJJ. Reducing power losses caused by ionic shortcut currents in reverse electrodialysis stacks by a validated model. *J Membr Sci*. 2008;310:418-430. <https://doi.org/10.1016/j.memsci.2007.11.032>.
12. Bjerrum N. Structure and properties of ice. *Dan Mat Fys Medd*. 1951;27:1-2.
13. Agmon N. The Grotthuss mechanism. *Chem Phys Lett*. 1995; 244:456-462. [https://doi.org/10.1016/0009-2614\(95\)00905-J](https://doi.org/10.1016/0009-2614(95)00905-J).
14. De Koning M, Antonelli A, Da Silva AJR, Fazzio A. Orientational defects in ice Ih: an interpretation of electrical conductivity measurements. *Phys Rev Lett*. 2006;96:075501. <https://doi.org/10.1103/PhysRevLett.96.075501>.
15. Petrenko VF, Whitworth RW. Structure of Ordinary Ice Ih—Part II: Defects in Ice—Volume 1: Point Defects, 1; 1994, pp. 1-35. <https://apps.dtic.mil/docs/citations/ADA280790>. Accessed March 1, 2019.
16. Petrenko VF. Electrical Properties of Ice; 1993.
17. H. Gränicher, C. Jaccard, P. Scherrer, A. Steinemann. Dielectric Relaxation and the Electrical Conductivity of Ice Crystals. *Discussions of the faraday society*. 1957;23:50-62. <https://doi.org/10.1039/DF9572300050>.
18. Aylward GH, Findlay TJV. *SI Chemical Data*. 6th ed. Australia: John Wiley & Sons; 2007.
19. Winger AG, Bodamer GW, Kunin R. Some Electrochemical Properties of New Synthetic Ion Exchange Membranes Some Electrochemical Properties of New Synthetic Ion Exchange Membranes I; n.d.
20. Długolecki P, Nijmeijer K, Metz S, Wessling M. Current status of ion exchange membranes for power generation from salinity gradients. *J Membr Sci*. 2008;319:214-222. <https://doi.org/10.1016/j.memsci.2008.03.037>.
21. Van Der Ham F, Witkamp GJ, De Graauw J, Van Rosmalen GM. Eutectic freeze crystallization simultaneous formation and separation of two solid phases. *J Cryst Growth*. 1999; 198-199:744-748. [https://doi.org/10.1016/S0022-0248\(98\)01003-3](https://doi.org/10.1016/S0022-0248(98)01003-3).

SUPPORTING INFORMATION

Additional supporting information may be found online in the Supporting Information section at the end of this article.

How to cite this article: Sleutels T, Kaniadakis I, Oladimeji O, van der Kooij H, ter Heijne A, Saakes M. An acid-doped ice membrane for selective proton transport. *Int J Energy Res*. 2020; 1-8. <https://doi.org/10.1002/er.6322>